



The photodetachment-modulated electron capture detector  
by Robert Stephen Mock

A thesis submitted in partial fulfillment of the requirements for the degree of Doctor of Philosophy in  
Chemistry

Montana State University

© Copyright by Robert Stephen Mock (1989)

Abstract:

Photodetachment (PD) of electrons from negative ions in a pulsed electron capture detector (ECD) is described. Sensitive responses to halogenated hydrocarbons that produce I-, Br-, or Cl- upon electron capture can be produced by passing a chopped light beam through the ECD and amplifying the modulated component of the signal. The photodetachment-modulated (PDM) ECD can be made to respond selectively and sensitively to iodine-containing hydrocarbons alone or to iodine- and bromine-containing hydrocarbons in the presence of chlorinated hydrocarbons. This capability is shown to be useful in the trace analysis of a complex mixture of halogenated hydrocarbons by gas chromatography. The PD spectra of Cl-, Br-, and I- and the absolute PD cross-section for I<sup>-</sup> at 365 nm are reported and are in excellent agreement with previous measurements by other methods.

Low resolution, electron PD spectra of the molecular radical anions of nitrobenzene and 30 other nitroaromatic hydrocarbons bearing methyl, fluoro, chloro, bromo, and cyano substituents are reported for the first time. Absolute PD cross-sections over the spectral range 300 to 1200 nm have been obtained. These molecules undergo PD by two mechanisms, Direct PD and Resonance PD. Through measurements of Direct PD, the minimum photon energy necessary to cause PD has been determined for each anion and compared with adiabatic electron affinities determined previously by gas phase electron transfer equilibria. Resonance PD spectra for many anions is compared to UV-Vis absorption spectra previously measured in gamma-irradiated frozen glasses. Through Resonance PD, peak maxima of high absolute cross-section are observed. Where the PD cross-section is small compared to the absorption cross-section at peak maxima, low quantum efficiency for Resonance PD is thought to result from poor Franck-Condon overlap.

By measuring the decrease in the PD response to azulene with increasing temperature, an electron autodetachment rate has been determined and is found to be consistent with previous results obtained in a pulsed high pressure mass spectrometer. The PDM-ECD has also been shown to be useful in determining the branching ratios of EC for CBrCl<sub>3</sub> and CCl<sub>4</sub>. Results also show that the neutral radicals, CCl<sub>3</sub> and CBrCl<sub>2</sub> . can undergo EC at low temperatures, but at higher temperatures are destroyed by well reactions

THE PHOTODETACHMENT-MODULATED  
ELECTRON CAPTURE DETECTOR

by

Robert Stephen Mock

A thesis submitted in partial fulfillment  
of the requirements for the degree

of

Doctor of Philosophy

in

Chemistry

MONTANA STATE UNIVERSITY  
Bozeman, Montana

March 1989

D378  
M717

APPROVAL

of a thesis submitted by

Robert Stephen Mock

This thesis has been read by each member of the thesis committee and has been found to be satisfactory regarding content, English usage, format, citations, bibliographic style, and consistency, and is ready for submission to the College of Graduate Studies.

2/24/89  
Date

Eric Dumsuel  
Chairperson, Graduate Committee

Approved for the Major Department

2/24/89  
Date

Edwin H. Abbott  
Head, Major Department

Approved for the College of Graduate Studies

3/9/89  
Date

Henry L. Parsons  
Graduate Dean

## STATEMENT OF PERMISSION TO USE

In presenting this thesis in partial fulfillment of the requirements for a doctoral degree at Montana State University, I agree that the Library shall make it available to borrowers under rules of the Library. I further agree that copying of this thesis is allowable only for scholarly purposes, consistent with "fair use" as prescribed in the U.S. Copyright Law. Requests for extensive copying or reproduction of this thesis should be referred to University Microfilms International, 300 North Zeeb Road, Ann Arbor, Michigan 48106, to whom I have granted "the exclusive right to reproduce and distribute copies of the dissertation in and from microfilm and the right to reproduce and distribute by abstract in any format."

Signature Robert Stephen Mark  
Date 2/24/89

## ACKNOWLEDGEMENT

I would like to thank the current and past members of the research group, especially Berk Knighton, Doug Zook, and Joe Sears, who were all tremendously helpful, and who are also good friends. I thank my advisor, Dr. Eric Grimsrud, for making my work here meaningful and productive. I thank my parents for instilling in me a life-long pursuit of learning, and for providing moral support. I thank my brother, Alan, for providing encouragement by "leading the way" through graduate school. Lastly, my gratitude to and love for Jan, Joshua, and Suzanne cannot be expressed in words. I thank them the most.

## TABLE OF CONTENTS

	Page
INTRODUCTION.....	1
THEORY.....	11
EXPERIMENTAL.....	21
RESULTS AND DISCUSSION.....	32
General Characterization of the PDM-ECD.....	32
Characterization of PD Response Perturbations.....	32
Effect of Chopping Frequency on PDM-ECD Perturbations.....	40
Measurement of PD Spectra for the Halide Anions.....	46
Measurement of an Absolute PD Cross-section for I <sup>-</sup> .....	48
Application of the PDM-ECD to Chemical Analysis.....	52
Use of PDM-ECD Responses for Chemical Analysis.....	52
Detection Limits of the PDM-ECD.....	56
Sensitivity of the PDM-ECD to CH <sub>3</sub> I in the Presence of Excess CCl <sub>4</sub> .....	58
PDM-ECD Study of Nitroaromatic Anions.....	61
PD Spectra of the Anions.....	61
Direct PD and Electron Affinities.....	72
Resonance PD.....	81
Phenoxy-type Ion Formation in the PDM-ECD.....	89
PDM-ECD Study of Quinone Anions.....	93
PD Spectra and EA of p-Benzoquinone.....	93
PD Spectra and EA of Chloranil and Fluoranil.....	97
PDM-ECD Study of Several Perfluorinated Compounds.....	99
PD of SF <sub>6</sub> .....	100
PD Spectra of Perfluorocycloalkanes.....	103
PD of Perfluorobenzene and Perfluorotoluene.....	104

TABLE OF CONTENTS-Continued

	Page
PDM-ECD Study of Azulene.....	106
PD Spectra of Azulene.....	108
Measurement of the Autodetachment Rate Constant of Azulene.....	110
Measurement of the Electron Attachment Rate Constant of Azulene.....	123
PDM-ECD Study of EC Chemistry of $CBrCl_3$ .....	128
Previous Studies.....	128
APIMS Measurements.....	130
PDM-ECD Measurements.....	133
Low Temperature Measurements.....	134
High Temperature Measurements.....	140
Application to Gas Phase Coulometry.....	145
Ion Location Experiment.....	146
SUMMARY.....	150
LITERATURE CITED.....	155
APPENDICES.....	162
Appendix A-Computer Simulation Program.....	163
Appendix B-Chromatographic Parameters.....	173

## LIST OF TABLES

	Page
1. Determination of the absolute photodetachment cross-section of iodide by PDM-ECD measurements at 365 nm.....	51
2. Photodetachment thresholds of nitroaromatic anions.....	70
3. Chromatographic parameters.....	174

## LIST OF FIGURES

	Page
1. Photodetachment spectra and cross-sections of iodide, bromide, and chloride negative ions.....	4
2. Theoretically predicted effects of photodetachment and its associated rate coefficients, $k_{hv}$ , on the $\delta I_{N'}$ , $\delta I_{L'}$ , $\delta I_{L/C'}$ , and $\delta I_{M'}$ responses.....	17
3. Predicted relationship between the ratio of the $\delta I_{M'}$ and $\delta I_{L/C'}$ responses and $k_{hv}$ .....	19
4. Apparatus used for the PD-pulsed ECD measurements...	21
5. Circuit diagram for the pulser and electrometer used for the PDM-ECD.....	26
6. Relative magnitude of light flux and minimum detectable PD cross-section.....	28
7. Chromatograms obtained from analysis using the four different response functions.....	34
8. Ratio of $\delta I_{M'}/\delta I_{L/C'}$ responses to (A) $CH_3I$ , (B) $CF_2Br_2$ , and (C) $CHCl_3$ observed with use of various relative intensities of light.....	38
9. Observed $\delta I_{M'}/\delta I_{L/C'}$ response ratios and phase angle offsets in the chromatographic analysis of $CH_3I$ , $CHCl_3$ , and $CCl_4$ as a function of chopper frequency..	41
10. Simulations of the two waveforms sent to the lock-in amplifier and the phase angle offset selected by the lock-in amplifier in order to provide a maximized output signal.....	43
11. $\delta I_{L/C'}$ and $\delta I_{M'}$ responses simultaneously observed in the repeated analysis of a sample containing $CF_2Br_2$ , $CH_3I$ , and $CHCl_3$ .....	47

## LIST OF FIGURES-Continued

	Page
12. Measured PD spectra of (A) iodide, (B) bromide, and (C) chloride.....	49
13. Chromatographic analysis of a mixture of 11 halogenated hydrocarbons.....	54
14. Two repeated analyses of a 5 cm <sup>3</sup> nitrogen gas sample containing 70 pptr CH <sub>3</sub> I, 4.5 ppb CHCl <sub>3</sub> , and 300 pptr CCl <sub>4</sub> .....	57
15. The relative PDM-ECD response ( $\delta I_M / \delta I_{L/C}$ ) to repeated 5 cm <sup>3</sup> gas injections of 600 pptr CH <sub>3</sub> I in a background matrix of CCl <sub>4</sub> .....	60
16. Repeated gas chromatographic analyses by the PDM-ECD of a sample containing 400 picograms of nitrobenzene.....	63
17. Electron photodetachment spectrum of the molecular anion of nitrobenzene.....	65
18. A simple model for the electron photodetachment of nitroaromatic anions.....	66
19. Electron photodetachment spectra observed for twelve substituted nitrobenzenes and dinitrobenzenes.....	67
20. Electron photodetachment spectra observed for twelve substituted nitrobenzenes and dinitrobenzenes.....	68
21. Electron photodetachment spectra observed for six substituted nitroaromatic and dinitroaromatic hydrocarbons.....	69
22. PD threshold energies, measured by the PDM-ECD, plotted against the adiabatic electron affinity (EA) of the corresponding nitroaromatic molecules.....	75
23. Possible resonance forms for (I) p-dinitrobenzene and (II) 1,5-dinitronaphthalene.....	78

## LIST OF FIGURES-Continued

	Page
24. The absorption spectra of the molecular radical anions of several nitroaromatic hydrocarbons.....	83
25. PD spectra of the three isomers of chloronitrobenzene.....	92
26. Spectra of p-benzoquinone.....	94
27. PD spectra of chloranil and fluoranil.....	98
28. PD spectra of SF <sub>6</sub> .....	101
29. Calculated potential energy curves of SF <sub>6</sub> and SF <sub>6</sub> <sup>-</sup> .....	102
30. PD spectra of four perfluorocarbons.....	105
31. PD spectrum of azulene.....	109
32. The apparent PD cross-section of azulene at 440 nm as a function of temperature.....	114
33. Relative PD cross-sections for I <sup>-</sup> and the p-fluoronitrobenzene anion as a function of temperature.....	115
34. Computer predictions of Rel σ vs. k <sub>d</sub> .....	119
35. Autodetachment rate coefficient, k <sub>d</sub> , for azulene as a function of temperature, determined with the PDM-ECD.....	120
36. Arrhenius plots of the rate constant, k <sub>d</sub> , for electron autodetachment from the azulene <sup>-</sup> negative ion.....	122
37. Relative normal ECD response to a constant 2 μg injection of azulene as a function of ECD temperature.....	125
38. Determinations of the electron attachment rate constant, k <sub>a</sub> , for azulene as a function of temperature.....	127

## LIST OF FIGURES-Continued

	Page
39. The relative abundance of $\text{Br}^-$ produced by atmospheric pressure EC reactions of $\text{CBrCl}_3$ observed over a wide range of temperatures.....	132
40. Relative abundance of $\text{Br}^-$ produced by electron capture of $\text{CBrCl}_3$ at $50^\circ\text{C}$ .....	137
41. Normal ECD responses to a repeated analysis of a sample containing $\text{CCl}_4$ , $\text{CH}_2\text{Br}_2$ , and $\text{CBrCl}_3$ as a function of temperature.....	143
42. The relative PD responses to iodide with light focused into the region of the ECD represented by the circles.....	148
43. Computer simulation program.....	169
44. Flow chart of computer simulation program.....	172

## ABSTRACT

Photodetachment (PD) of electrons from negative ions in a pulsed electron capture detector (ECD) is described. Sensitive responses to halogenated hydrocarbons that produce  $I^-$ ,  $Br^-$ , or  $Cl^-$  upon electron capture can be produced by passing a chopped light beam through the ECD and amplifying the modulated component of the signal. The photodetachment-modulated (PDM) ECD can be made to respond selectively and sensitively to iodine-containing hydrocarbons alone or to iodine- and bromine-containing hydrocarbons in the presence of chlorinated hydrocarbons. This capability is shown to be useful in the trace analysis of a complex mixture of halogenated hydrocarbons by gas chromatography. The PD spectra of  $Cl^-$ ,  $Br^-$ , and  $I^-$  and the absolute PD cross-section for  $I^-$  at 365 nm are reported and are in excellent agreement with previous measurements by other methods.

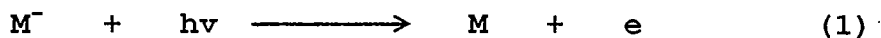
Low resolution, electron PD spectra of the molecular radical anions of nitrobenzene and 30 other nitroaromatic hydrocarbons bearing methyl, fluoro, chloro, bromo, and cyano substituents are reported for the first time. Absolute PD cross-sections over the spectral range 300 to 1200 nm have been obtained. These molecules undergo PD by two mechanisms, Direct PD and Resonance PD. Through measurements of Direct PD, the minimum photon energy necessary to cause PD has been determined for each anion and compared with adiabatic electron affinities determined previously by gas phase electron transfer equilibria. Resonance PD spectra for many anions is compared to UV-Vis absorption spectra previously measured in gamma-irradiated frozen glasses. Through Resonance PD, peak maxima of high absolute cross-section are observed. Where the PD cross-section is small compared to the absorption cross-section at peak maxima, low quantum efficiency for Resonance PD is thought to result from poor Franck-Condon overlap.

By measuring the decrease in the PD response to azulene with increasing temperature, an electron autodetachment rate has been determined and is found to be consistent with previous results obtained in a pulsed high pressure mass spectrometer. The PDM-ECD has also been shown to be useful in determining the branching ratios of EC for  $CBrCl_3$  and  $CCl_4$ . Results also show that the neutral radicals,  $CCl_3$  and  $CBrCl_2$ , can undergo EC at low temperatures, but at higher temperatures are destroyed by wall reactions.

## INTRODUCTION

Since its introduction in the 1950's, the electron capture detector (ECD) has been the most common gas chromatographic (GC) detector for the determination of environmental samples. This is due to the fact that the gas-phase electron attachment rates for many molecules of environmental interest are very fast while the attachment rates for many hydrocarbons, a large but uninteresting portion of most environmental samples, are relatively slow. The ECD can then provide a sensitive and selective detection technique requiring a minimum of sample clean-up or preparation. For example, detection and measurement of atmospheric halocarbons in relatively clean air has been accomplished by GC-ECD by injections of whole air samples (1-3). More complicated samples containing tens or hundreds of hydrocarbons with significant electron capture coefficients can create more of a detection problem. The inherent selectivity of the ECD may not be enough to provide accurate identification of the compounds present. In such cases, a more selective or intelligent detection system must be used, such as mass spectrometry.

Recently, the versatility of the ECD for a wide variety of analyses has been greatly improved by what may collectively be called the chemically sensitized (CS) ECD. By the intentional addition of oxygen (4, 5) or nitrous oxide (6) to the carrier gas, the ECD can respond to classes of compounds which do not capture electrons rapidly under normal conditions. The intentional addition of ethyl chloride to the carrier gas has been shown to enhance the ECD response to compounds of low electron affinities, such as anthracene (7). Although the CS-ECD improves the sensitivity to some classes of compounds, it is not yet known whether chemical sensitization will assist in the analysis of complex samples. What is needed for complex samples is an induced perturbation of the ECD signal, which, when detected and amplified, provides an additional element of specificity towards sample components of interest. One means of creating a perturbation of this type is the introduction of light-induced photodetachment (PD), Reaction 1, into the ECD. Ideally, this electron



capture-photodetachment detector would respond only to those compounds which 1) rapidly capture thermalized electrons, and 2) form negative ions which will readily undergo photodetachment at a selected wavelength.

Electron photodetachment from atomic and polyatomic anions has proven to be a useful means of studying thermochemical and spectroscopic properties of negative ions and their photoproducts (8-12). The photodetachment spectra of numerous atomic (13-18) and polyatomic (19-26) negative ions have previously been reported. The PD process is a transition from a bound electron in the anion to a free continuum electron and the neutral. The minimum energy required to induce PD is equal to the electron affinity (EA) of the neutral. Hence, PD has been extensively used for the measurement of gas phase electron affinities (27). Since electron affinities seldom exceed 4 eV, visible and near-UV light sources can be used to induce PD. The PD spectra of polyatomic negative ions has also been shown to provide information concerning the excited states of the negative ions and the neutral products.

Photodetachment spectra are often broad and relatively featureless. For atomic negative ions, such as the halides shown in Figure 1, the increase in cross-section,  $\sigma$ , with photon energy is very abrupt in the region of the EA-determined threshold. The most significant difference between the PD spectra of  $I^-$ ,  $Br^-$ , and  $Cl^-$  shown in Figure 1 is the differing onsets of PD corresponding to the EA of each halide ion.

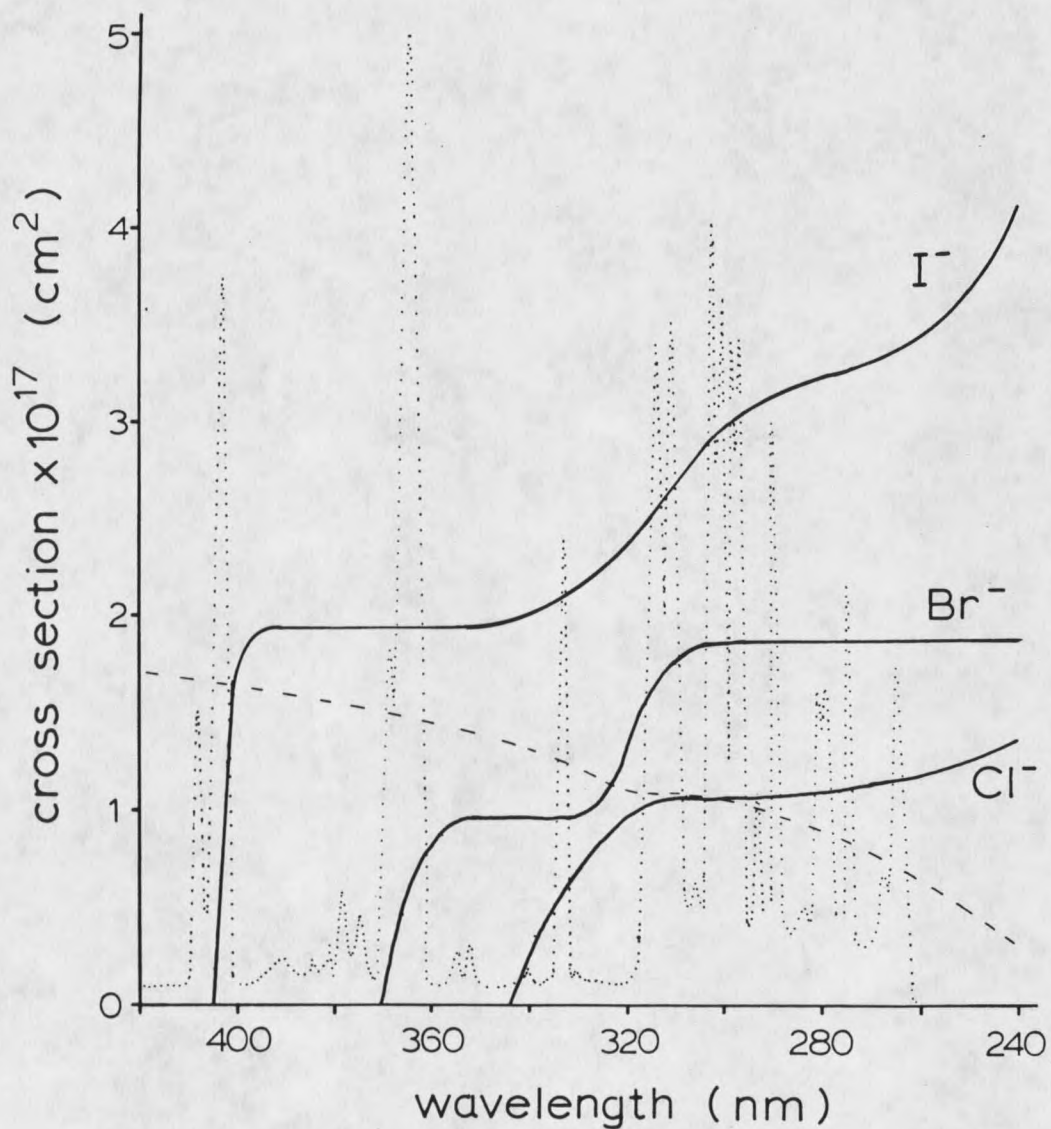


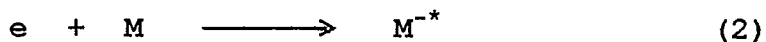
Figure 1. Photodetachment spectra and cross-sections of iodide, bromide, and chloride negative ions (reproduced from references 13 and 14). Also shown are the emission spectra of a Xe (dashed line) and a Hg/Xe (dotted line) arc lamp.

The PD spectra of polyatomic anions tend to exhibit a gradual increase in  $\sigma$  with increasing photon energy in the threshold region. This gradual increase is expected due to the added complexities associated with the numerous vibronic and rotational states that are accessible to the polyatomic anion and the neutral product. Also, differences in the geometries of the negative ion and the neutral ( Franck-Condon overlap) can greatly complicate the PD spectra of polyatomic anions.

In the previously mentioned studies of PD, measurements were generally made by one of two approaches. For most studies involving atomic anions, measurements were made utilizing shock tubes. For example, Mandl (13, 14) introduced cesium halides into nitrogen gas and subjected the gas sample to shock heating, causing the cesium halide to ablate and dissociate, forming positive ions and negative halide ions. This method produces very high ion densities, on the order of  $10^{16}$  ions/cm<sup>3</sup>. Ultraviolet light produced by a Xe flash lamp is introduced into the shock tube containing the ions and the absorption of light measured. The absorption is due to PD of the negative halide ions; so the magnitude of the absorption is proportional to the PD cross-section of the anion.

For polyatomic anions, the most common approach has been that involving the ion cyclotron resonance mass

spectrometer (ICR-MS) in conjunction with a light source (8, 11). This technique involves the measurement of the diminution by light of mass spectrometrically generated ion beams. Although the ICR-MS is well-suited to the study of PD due to its ability to generate a variety of mass-identified negative ions and then to trap and study them for relatively long periods of time, there are certain inherent limitations. First, the internal energy of the negative ions produced in an ICR cavity is generally not under tight experimental control, which can complicate the interpretation of PD spectra (8, 11). The negative ions are typically formed by energetic chemical means and the excess internal energy imparted to the product ions is not efficiently removed by collisions in the  $10^{-8}$  to  $10^{-5}$  Torr environment of the ICR cavity (28-30). This is especially severe when an anion is formed by resonance electron capture, Reaction 2, from a molecule, M, of high electron affinity. Since the EA of



molecules which readily lead to negative ions can be quite high, occasionally exceeding 3eV, the internal energy imparted to the molecular anion,  $M^{-*}$  by Reaction 2 will be correspondingly high.

A second problem can arise in ICR-MS photodetachment studies if the natural lifetime of the initially-formed

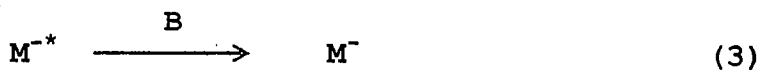
excited anion,  $M^{-*}$ , is too short against autodetachment, the reverse of Reaction 2. For example, Christophorou (31) has shown that the lifetimes of the molecular negative ions of nitrobenzene and substituted nitrobenzenes formed by capture of low-energy electrons are on the order of tens of microseconds. Since stabilizing collisions can occur in an ICR cavity no faster than about one per millisecond, the natural lifetimes of these initially-formed negative ions may not be sufficiently long as to allow their PD spectra to be reliably measured. Perhaps for this reason, the PD spectra of only a few molecular radical anions have been reported by the ICR method. If the lifetime is sufficiently long, a PD spectrum may be obtained. An example is the study of the resonance electron capture product of  $SF_6$ . For this anion, a PD experiment was reported by the ICR-MS (32) and appears to have been made possible by the existence of one of several excited states of  $SF_6^{-*}$  which has an unusually long lifetime against autodetachment (31, 33-35). Most of the PD measurements of polyatomic negative ions reported by the ICR-MS method have been performed on negative ions formed by dissociative electron capture reactions or by ion-molecule reactions in which an even electron anion is irreversibly formed.

In 1983, Dovichi and Keller (36) described the use of an ECD for the measurement of the PD spectrum of  $\text{NO}_2^-$  at atmospheric pressure. In that experiment, a line-tunable argon-ion laser producing up to 3W of continuous power in the selected wavelengths was used in conjunction with a direct current (DC) ECD. With this instrument, PD-modulated (PDM) ECD responses to  $\text{NO}_2^-$  were observed. Although the PDM signals were weak, they were sufficiently strong as to provide a PD spectrum of  $\text{NO}_2^-$  that was consistent with the known PD spectrum. In that study, the low PDM-ECD sensitivity can be partially attributed to the small PD cross-section for  $\text{NO}_2^-$  at the wavelengths used; at 488 nm,  $\sigma = 4 \times 10^{-19} \text{ cm}^2$  (26). Also, low sensitivity may have resulted from the use of a DC-ECD. The basic operational principles of a DC-ECD are not well understood (37). In particular, the location and lifetimes of negative ions within a DC-ECD are unknown.

With a pulsed ECD, it is possible to describe more clearly the dynamics occurring within the ionization volume. Several details of this description point to potential advantages of the pulsed ECD over the DC-ECD for its application to PD. For example, it is known that the lifetimes of the negative ions formed within a pulsed ECD are relatively long and these ions will be concentrated in a predictable location within the

ionization volume by a positive ion-space charge field (38, 39). If a cylindrical ionization cell is used, the negative ions formed will be contained along its central axis (39). If a light beam is then passed through this same region of the cell, the interaction of negative ions and photons will be maximized. Since most of the important ECD processes which effect the measured electron current can be modeled with a reasonable level of accuracy, a relatively detailed understanding of the quantitative response of the PDM-pulsed ECD should be possible. Using these models, it may be possible to determine absolute, as well as relative, PD cross-sections for negative ions formed in the ECD.

There are also inherent advantages to using the PDM-pulsed ECD specifically for the PD studies of molecular anions. In particular, the molecular anions of nitroaromatic hydrocarbons are readily formed in an ECD by electron capture, Reaction 2. These excited state molecular anions are then rapidly quenched by collisions with the atmospheric pressure buffer gas, B, as shown in Reaction 3. This process overwhelms autodetachment, the

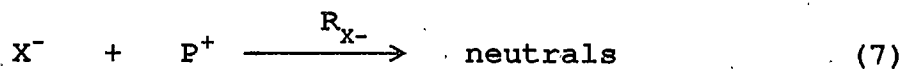
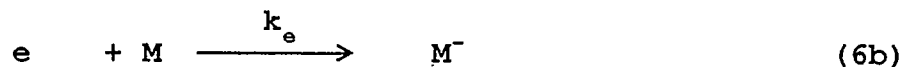
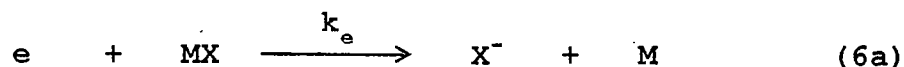
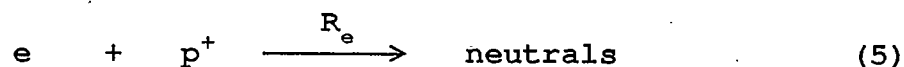


reverse of reaction 2. Also, at atmospheric pressure, Reaction 3 is sufficiently effective in removing excess internal energy from the negative ions that the ions are

almost certainly in thermal equilibrium with the buffer gas. This should greatly simplify the interpretation of PD spectra and allow meaningful comparisons between PDM-pulsed ECD results and those of previous studies of the thermodynamic and spectroscopic properties of the corresponding ground state anions.

## THEORY

With a thorough understanding of the processes occurring within the ECD, it should be possible to predict and understand the qualitative and quantitative responses to various molecules. The model to be discussed here is the same as models for the pulsed ECD described elsewhere (38, 40) with the addition of the photodetachment reaction. The important reactions occurring within the ECD which should adequately explain and determine the magnitude of the electron population between pulses are shown as Reactions 4-8.



The ion chemistry occurring within the ECD is initiated by continuous beta radiation emitted by a  $^{63}\text{Ni}$ -

on-Pt foil which forms the cylindrical walls of the cell (38). The secondary electrons created by this radiation are rapidly thermalized in the atmospheric pressure buffer gas and are contained within the central region of the reaction volume by a positive ion space-charge field (38, 39). The rate coefficient,  $\beta$ , for this process is found by measuring the maximum standing current obtained at a very rapid pulse frequency in the absence of sample (41). In the ECD used in this study,  $\beta = 1.87 \times 10^{10}$  ion pairs  $s^{-1}$ . A measure of the average electron density existing within the cell is continuously provided by the fixed-frequency, pulsed method of ECD operation (38) in which all free electrons are periodically collected at the anode by a positive voltage pulse.

Reaction 5 is the recombination of electrons with positive ions. For a given detector, the product of the rate coefficient,  $R_e$ , and the positive ion density,  $n_+$ , can be determined from measurements of standing current as a function of pulse frequency (41). For this detector at  $100^\circ\text{C}$ ,  $R_e n_+ = 300 \text{ sec}^{-1}$ .

When a molecule of high electron affinity enters the cell, some of the electrons will be captured to form stable negative ions. Reaction 6a represents dissociative electron capture, which, in this study, leads to the formation of  $I^-$ ,  $Br^-$ , or  $Cl^-$ . Resonance electron capture is represented by Reaction 6b. In this

case, which is actually the sum of Reactions 2 and 3, stable molecular ions are formed. (In the following discussion of the kinetic fate of the negative ions,  $X^-$  will be used as the negative ion representation. However, the molecular ion  $M^-$  has the same fate. Later, when the spectra of the ions are addressed, distinctions will be made as to exact identity.) Both Reactions 6a and 6b will decrease the average electron population within the cell. The first order rate of electron loss by either Reaction 6a or 6b will be given by the product,  $k_e n_{mx}$ . The negative ions formed will also be contained within the central region of the ECD by the positive ion space charge and will not be lost by non-chemical means such as wall neutralization or ventilation out of the cell.

In the absence of light, all negative ions will be lost by recombination with positive ions, represented by Reaction 7. The pseudo-first-order rate coefficient,  $R_{x^-n_+}$ , will be of major importance in predicting the magnitude of PD perturbations of the ECD response since Reaction 7 and Reaction 8 will compete directly for the available negative ions,  $X^-$ . If destruction of  $X^-$  occurs by Reaction 7, only neutrals are formed, and the loss of an electron from the system caused by Reaction 6 will be measured by the electrometer. If, however,  $X^-$  is destroyed by Reaction 8, an electron is regenerated and

the electron capture event is not detected by the electrometer.

The rate coefficient,  $R_{x-n_+}$ , for Reaction 7 cannot be measured directly by an ECD. An estimate of its magnitude can be made, however, based on the measurement of  $R_{e-n_+}$  from Reaction 5. Prior studies of atmospheric pressure ionization in a  $^{63}\text{Ni}$  source have shown an increase in total positive ion density whenever the source is altered from an electron-dominated to a negative ion-dominated system by the introduction of a high concentration of an electron capturing substance (5, 42). The magnitude of this increase in total positive ion signal has been between 50 and 100%. This effect appears to be independent of the electron capturing substance used. Since the density of positive ions within a field-free atmospheric pressure ion source is thought to be determined by recombination reactions, the above observations should reflect the relative magnitudes of  $R_e$  and  $R_{x-}$ . More precisely, the total positive ion densities should be inversely proportional to the square root of the recombination coefficients involved (38, 42). These observations then lead to the following estimate:  $R_{x-}$  is expected to be one-half to one-fourth as large as  $R_e$ . This is consistent with other data. At atmospheric pressure, ion-ion recombination coefficients tend to a constant value of about  $1 \times 10^{-6} \text{ cm}^3 \text{ s}^{-1}$  (43). Positive

ion-electron recombination coefficients can exceed this value if the positive ions are cluster ions. The electron recombination coefficients of the cluster ions,  $H^+(H_2O)_2$  and  $H^+(H_2O)_3$ , are  $2 \times 10^{-6}$  and  $4 \times 10^{-6} \text{ cm}^3 \text{ s}^{-1}$ , respectively (44, 45). Cluster ions of the type  $H^+(H_2O)_n$  are commonly observed in atmospheric pressure ion sources (46), and the two cluster ions indicated, where  $n=2$  and  $n=3$ , are the ones expected in relatively dry carrier gas. The following assessment now seems reasonable: when a small amount of MX enters the ECD, the small population of  $X^-$  which is created will recombine with positive ions at a rate described by  $R_{X^-n^+} \approx 1/3 R_{e n^+}$ . Since  $R_{e n^+}$  in this ECD is  $300 \text{ s}^{-1}$ , a reasonable approximation is that  $R_{X^-n^+} = 100 \pm 50 \text{ s}^{-1}$ .

The rate coefficient for Reaction 8 is given by  $k_{hv} = \sigma\Phi$ , where  $\sigma$  is the PD cross section and  $\Phi$  is the light flux. If a negative ion, such as  $I^-$  shown in Figure 1, has  $\sigma = 2 \times 10^{-17} \text{ cm}^2$  and is irradiated with  $1.0 \text{ W cm}^{-2}$  of 380 nm light ( $\Phi = 2.0 \times 10^{18} \text{ photons cm}^{-2} \text{ s}^{-1}$ ), then  $k_{hv} = 40 \text{ s}^{-1}$ . Comparing this  $k_{hv}$  value to  $R_{X^-n^+} = 100 \text{ s}^{-1}$ , it is clear that reaction 8 can compete effectively with Reaction 7. In this particular case, almost one-third of the negative ions,  $X^-$ , will be photodetached by the light. This large a perturbation of the ECD processes should be easily measurable.

The expected response perturbations when PD is introduced into the ECD are shown in Figure 2 and are plotted as a function of the magnitude of  $k_{hv}$ . Although the magnitudes of the  $k_{hv}$  values shown are relatively large, the lower portion of the range should be readily achievable for favorable systems. Four types of ECD responses are shown in Figure 2, all of which can be measured with the instrumentation to be described in the Experimental Section.  $\delta I_N$  is the normal ECD response expected with no light present.  $\delta I_L$  is the response expected when a beam of light is continuously passed through the ECD.  $\delta I_M'$  is the PD-modulated component of the ECD response expected when a chopped light beam passes through the cell. In the calculation of  $\delta I_M'$ , it is assumed that the dynamic processes occurring within the ECD are on a very fast time scale compared to the chopping frequency. The actual PD-modulated response,  $\delta I_M$ , is not identical to the predicted  $\delta I_M'$ . This issue will be addressed later. From Figure 2, it is seen that  $\delta I_M' = \delta I_N - \delta I_L$ .  $\delta I_{L/C}$  is the ECD response expected when a chopped light beam is passed through the cell.  $\delta I_{L/C}$  is equal to the average of  $\delta I_N$  and  $\delta I_L$ , and closely approximates  $\delta I_N$  when  $k_{hv}$  is small. All of the predicted responses were calculated with a personal computer by numeric integration of the processes described in Reactions 4-8 using the previously stated rate

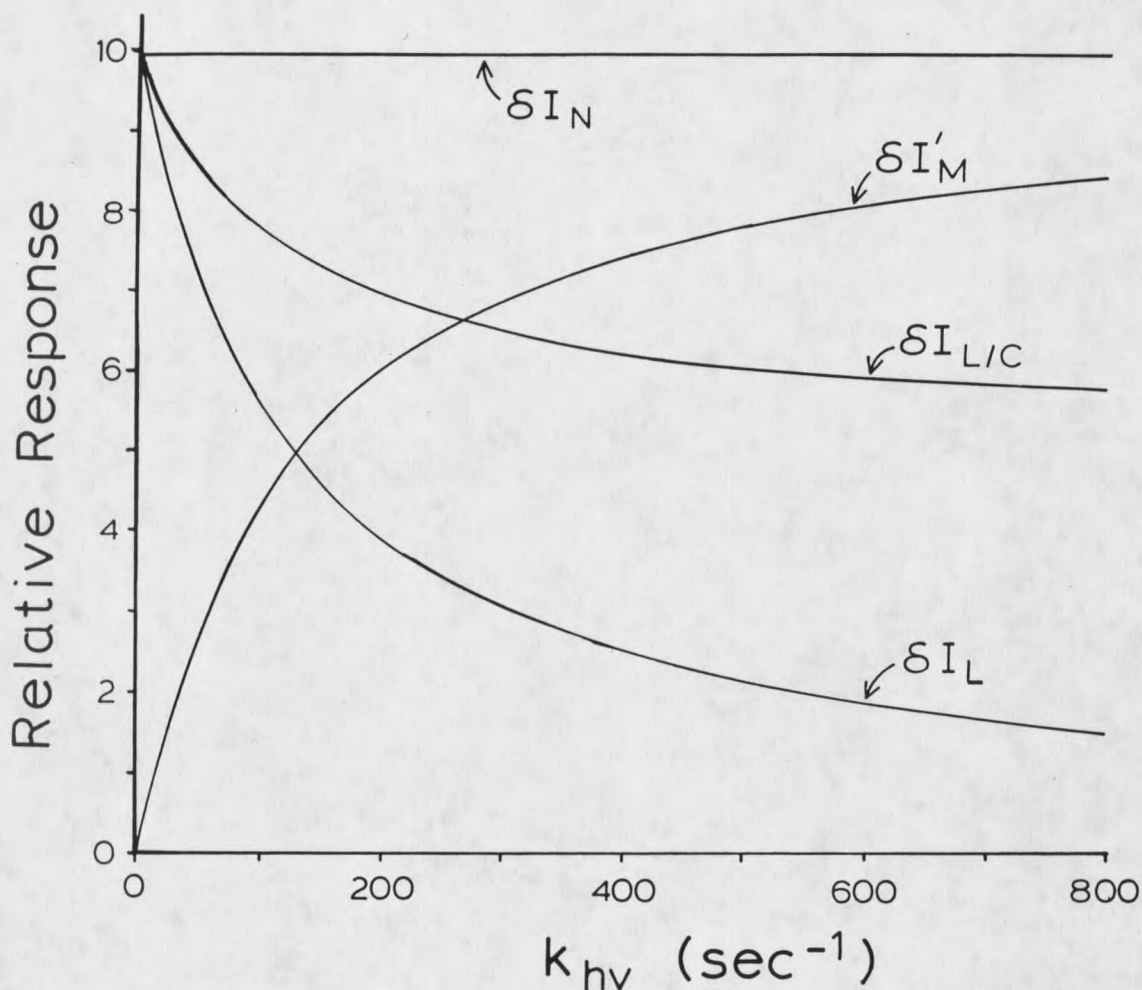


Figure 2. Theoretically predicted effects of photo-detachment and its associated rate coefficient,  $k_{hv}$ , on the  $\delta I_N$ ,  $\delta I_L$ ,  $\delta I_{L/C}$ , and  $\delta I'_M$ , responses of the pulsed ECD. Calculated from a model including Reactions 4-8 for which the following rate coefficients were used:  $B = 1.87 \times 10^{10}$  ion pairs  $\text{s}^{-1}$ ,  $R_{n+} = 300 \text{ s}^{-1}$ ,  $R_{x-n+} = 100 \text{ s}^{-1}$ . While  $k_{n+} = 100 \text{ s}^{-1}$  and a pulse frequency of 2 kHz are used, predictions of relative responses are independent of the magnitudes chosen for these parameters.

coefficients. A description of the program, along with a flow-chart and listing, are provided in Appendix A. Although values of  $k_e n_{e, \text{max}} = 100 \text{ s}^{-1}$  and a pulse frequency of 2KHz were used in these calculations, the results are independent of these parameters. Boundary conditions used in these calculations are that the population of electrons grows during each period between electron-removing pulses from zero to some positive value, and that the population of negative ions is the same at the beginning and end of each pulse period. In these calculations, the choice of sample size has no effect on the relative responses indicated in Figure 2 as long as sample size is kept small, so that no  $\delta I$  responses greater than 10% of the standing current occur. Within this low-sample range, all responses are predicted to be proportional to sample concentration.

Figure 2 predicts that over most of the range of  $k_{hv}$  values shown, PD should induce very significant and easily measurable perturbations of ECD responses. The magnitude of the modulated response,  $\delta I_M'$ , can easily be made 10% as great as the normal ECD response,  $\delta I_N$ . At higher  $k_{hv}$  values, the predicted response curve for  $\delta I_M'$  becomes less steep and additional increases in light intensity have smaller effects.

In curve A of Figure 3, the ratio of the predicted  $\delta I_M'$  and  $\delta I_{L/C}$  responses are plotted as a function of

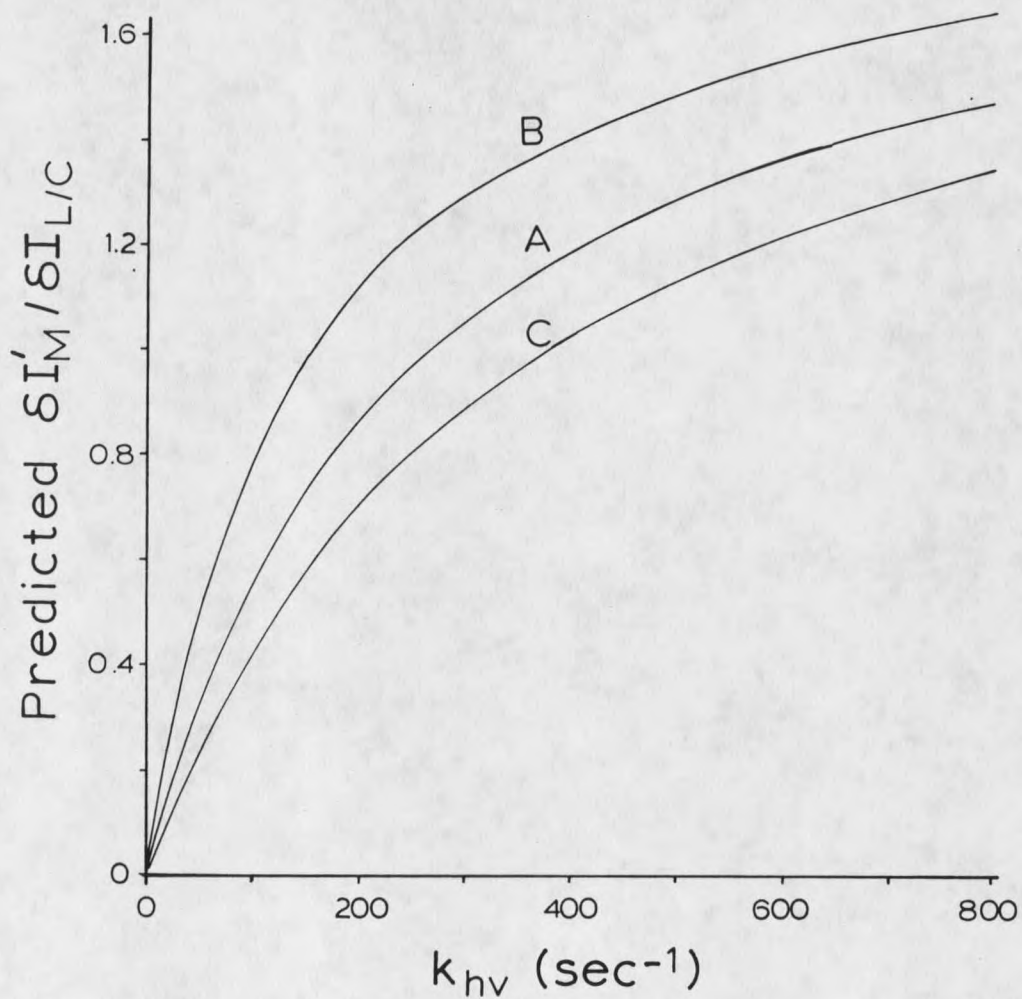


Figure 3. Predicted relationship between the ratio of the  $\delta I_M'$  and  $\delta I_{L/C}$  responses and  $k_{hv}$ . Rate coefficients used are those listed in Figure 2 except the values chosen for the negative ion recombination coefficient,  $R_{X-n+}$ , are (A) 100, (B) 50, and (C) 150 s<sup>-1</sup>.

$k_{hv}$ . The ratio of these two responses is of special interest since it can be obtained simultaneously in an experiment utilizing a chopped light beam. These two responses should also provide a more accurate measure of the processes occurring within the ECD than a comparison of ECD responses with light continuously on or off since bulk heating of the source gas by the intense light (36) can be minimized in a chopped-light experiment. From Figure 3, the ratio of  $\delta I_M'$  to  $\delta I_{L/C}$  is predicted to be a sensitive function of the rate coefficient,  $k_{hv}$ , for Reaction 8. The ratio may provide a means of determining  $k_{hv}$  and also  $\sigma$  if  $\Phi$  can be accurately measured. The accuracy of the method for determining  $k_{hv}$  is dependent upon the accuracy of the value for  $R_{x-n_+}$ . As described earlier, a value of  $R_{x-n_+} = 100 \pm 50 \text{ s}^{-1}$  seems reasonable. In Figure 3, curves B and C represent the predicted ratios for  $R_{x-n_+} = 50$  and  $150 \text{ s}^{-1}$ , respectively.























































































































































































































































































































